NJC

Accepted Manuscript

This article can be cited before page numbers have been issued, to do this please use: Y. Tang, H. Gao, M. Yang, G. Wang, J. Li, H. Zhang and Z. Tao, *New J. Chem.*, 2016, DOI: 10.1039/C6NJ01654E.

View Article Online
DOI: 10.1039/C6NJ01654E

Journal Name

ARTICLE

NiO Promoted CuO-NiO/SBA-15 Composites as Highly Active Catalysts for Epoxidation of Olefins

Yinhai Tang, Hongyi Gao, Mu Yang*, Ge Wang*, Jie Li, Huan Zhang, Zhang Tao

Received 00th January 20xx,
Accepted 00th January 20xx

DOI: 10.1039/x0xx00000x

www.rsc.org/

In this paper, CuO-NiO supported on mesoporous silica SBA-15 was developed using the ultrasonic post-grafting method. The bi-metallic oxides are well-dispersed in very small sizes in the mesoporous channels, and the presence of NiO enhances the surface content of CuO, leading to a redistribution of CuO and the well dispersion of CuO nanoparticles, which were characterized by high-resolution transmission electron microscopy (HRTEM), XRD and N_2 absorption and desorption isotherms examinations. In comparison with the CuO/SBA-15 or NiO/SBA-15, the electron transfer that occurs between the two metals oxide and high dispersion of the active components improves the overall selective oxidation of olefin.

1. Introduction

Selective oxidation of olefin is of crucial importance in the synthesis of fine chemicals and intermediates.[1-4] One example is styrene, while styrene epoxide is an important intermediate for the synthesis of complex components for commercial procedures. For instance, it can be used for the production of chiral aziridines with retain their configuration,[5] as well as chiral ring-opened products with alcohols[6] and amines,[7] etc., due to the ease with which epoxide ring reacts with a wide range of uncleophiles.[8-10] However, the diverse oxidation pathway of styrene causes many other products makes selective epoxidation difficult.[11-13]

Nowadays, much attention has been paid to the transition-metal oxides heterogeneous catalysts for the selective oxidation of olefin.[14-16] Among these, copper oxide has been employed in a variety of processes due to its low-cost, being naturally abundant, having good catalytic performance and being environmentally friendly.[17,18] However, the aggregation and restructuring of the CuO nanoparticles still limit their application. Recently, copper oxide is introduced into or encapsulated with ordered mesoporous materials since their various pore structures and large surface area favor the catalytic nanoparticles dispersal and stablility.[19] For example, Chen et al. coated CuO nanoclusters with mesoporous SiO_2 using the one-pot solvothermal synthetic method, which showed higher activity and stability in olefin epoxidation reaction than that of commercial CuO.[20] However, the unique catalytic sites still have the drawback of relative-low catalytic activity or overoxidation. Given these limitations, hybrid catalysts have attracted widespread interest because of their markedly better properties than those of either of the constituent metal oxides.[21] Ravasio et al. synthesized a bifunctional supported copper catalyst CuO/Al_2O_3, which showed an excellent catalytic property for the one-pot epoxidation of alkenes.[22] Ye et al. deposited CuO nanoparticles on the surface of Ag nanowires, and the novel CuO@Ag nanowires showed a synergistic effect, leading to outstanding catalytic activities in the epoxidation of trans-stilbene under mild reaction condition.[23] Our group prepared a hybrid Fe_3O_4-CuO@meso-SiO_2 catalyst using a multi-step assembly method, and the meso-structure and multiple functionalities (Fe_3O_4-CuO) showed high selectivity for styrene oxide.[24]

Recently, a new bimetallic oxide system of CuO-NiO has been developed,[25,26] which has many applications in catalytic processes. It is well known that heterogeneous copper catalysts are effective in oxidation, while the presence of traces of nickel oxide ensures an improved and stabilization of copper.[27,28] Among those researches, a CuO-NiO system has been studied in selective hydrogenation and dehydrogenation, while its application for the epoxidation of olefins is the subject of ongoing research.

In this paper, we report a NiO promoted CuO-NiO/SBA-15 composites synthesized via the ultrasonic post-grafting method. With the assistance of -NH_2 groups on the SBA-15 internal surfaces, the precursors were absorbed into the mesoporous channels easily under ultrasonic conditions. The presence of NiO improved the dispersion of CuO-NiO in the mesoporous channels, giving significantly improved activity for the epoxidation of olefins with a remarkably high selectivity. Moreover, the increase of a small amount of NiO promotes the overall catalytic performance of the catalysts.

Beijing Key Laboratory of Function Materials for Molecule & Structure Construction, School of Material Science and Engineering, University of Science and Technology Beijing, Beijing, 30 Xueyuan Road, 100083, P. R. China. E-mail: yangmu@ustb.edu.cn; gewang@mater.ustb.edu.cn

† Electronic Supplementary Information (ESI) available: [FT-IR, TGA and HRTEM]. See DOI: 10.1039/x0xx00000x

DOI: 10.1039/C6NJ01654E

2. Experimental

2.1 Materials.

Cupric nitrate ($Cu(NO_3)_2$ $3H_2O$), nickel nitrate ($Ni(NO_3)_2$), tetraethyl-orthosilicate [$(OC_2H_5)_4Si$, TEOS], tert-butyl hydroperoxide (TBHP) and HCl (36-38 wt.%) were purchased from Beijing Chemical Reagent Company. Pluronics P123 (Mw = 5800) and all of the olefins were supplied by SigmaeAldrich and Alfa Aesar, respectively. All reagents were used as received without further purification.

2.2. Preparation of modified SBA-15.

First, the SBA-15 was synthesized following previously reported methods.[16] In a typical procedure, P123 (4.0 g) as the structure-directing agent was first dissolved in 30 mL H_2O at 35 ℃, and 120 mL 2.0 M HCl aqueous solution was added. Tetraethyl-orthosilicate (TEOS, 8.5 g) was added dropwise as the silica source, and the mixture was stirred at 35 ℃ for 24 h. The resultant gel was transferred into a Teflon-sealed autoclave and heated to 110 ℃ for 24 h. After cooling down, the precipitate was recovered and washed with de-ionized water several times. The obtained SBA-15 with template was then dried at 80 ℃ overnight for further modification.

The obtained SBA-15 was modified with $-CH_3$ and $-NH_2$ according to our reported procedure.[29] In a typical procedure, as-prepared SBA-15 (2.0 g) was dispersed into dry toluene (150 mL) under nitrogen atmosphere. Then 10 mL of trimethylchlorosilane (TMCS) was added dropwise, and the mixed solution was stirred at 80 ℃ for 8h under reflux. After that, the solid was filtered and washed with toluene and alcohol several times, and then calcined at 350 ℃ for 6 h to remove the structure-directing agent P123. Then, the obtained sample (2.0 g) was dispersed into 150 mL dry toluene, and 6.0 mL 3-aminopropyltriethoxylsilane (APTES) was added dropwise. The mixed solution was stirred at 25 ℃ for 12 h and refluxed at 80 ℃ for another 8 h. Then the solid was collected and dried at 60 ℃ for 8 h, and the modified SBA-15 was obtained.

2.3. Preparation of CuO-x NiO/SBA-15 composites.

CuO-NiO/SBA-15 composites were prepared via the ultrasonic post-grafting method.[30] Modified SBA-15 (0.2 g) was first dried at 120 ℃ for 4 h in a vacuum condition in order to remove the adsorbed water. Then 20 mL $Cu(NO_3)_2$ $3H_2O$ (1.61 g) and $Ni(NO_3)_2$ (0.97 g) ethanol solution (the total concentration of the metal ions being 0.5 M) was injected into the vacuum system under ultrasonic conditions. After 4 h of ultrasonic impregnation, the solid was filtered and washed with ethanol several times. The obtained composite was dried at 60 ℃ overnight and calcined at 550 ℃ for 4h with a heating ratio of 2 ℃/min. The final CuO-NiO/SBA-15 composites were obtained and named as CuO-x NiO/SBA-15 (x represents the molar ratio of Ni/Cu, according to the ICP analysis)

To investigate the influence of the amount of NiO, CuO-NiO/SBA-15 with higher NiO loading was prepared by using the ultrasonic post-grafting method without filtering the precursor off during the synthesization process.

2.4. Characterization.

The Fourier-transform infrared (FT-IR) spectra were examined using a Nicolet 6700 spectrometer. The morphology and structure of CuO-x NiO/SBA-15 was examined using high-resolution transmission electron microscopy (HRTEM) on a JEM-2100F equipped with an energy-dispersive X-ray (EDX) operated the accelerating voltages of 200 kV. The crystalline phases were analyzed by XRD pattern on a M21X diffractometer (MAC Science Co. Ltd., Japan) using a Cu Ka radiation (λ = 1.541 Å) source at 40 kV and 200 mA. Nitrogen adsorption-desorption isotherms were obtained using an AUTOSORB-1C analyzer (USA Quantachrome Instruments) at 77 K, and the specific surface area was measured using the Brunauer-Emmett-Teller (BET) method. Pore size distributions were calculated using the Barrett-Joyner-Halenda (BJH) method from the adsorption branches of the isotherms. Cu and Ni elemental analysis was performed by inductively coupled plasma-atomic emission spectrometry (ICP-AES) using a Vavian 715-ES. X-ray photoelectron spectroscopy (XPS) data was obtained with an Escalab 220i-XL electron spectrometer from VG Scientific using 300W Al Ka radiation. Finally, the catalytic properties were analyzed by Agilent 7890/5975C-GC/MSD.

2.5. Catalytic properties.

The catalytic epoxidation of styrene was performed in a two-necked round-bottom flask fitted with a reflux condenser. First, the catalyst containing 0.0129 mmol of CuO, 5.0 mL acetonitrile, 3.0 mmol of styrene and 0.02 mL of nitrobenzene as internal standard for GC-MS analysis were mixed within the flask and the reaction temperature was maintained at 80 ℃. Then 5 mmol of tert-butyl hydroperoxide (TBHP) was added drop-wise under vigorous stirring. After a desired time, the catalyst was collected and the liquid phase was analyzed by gas chro-matography-mass spectrometry (HP-5 column, Ar carrier gas, 200 ℃).

To confirm the wider applicability of our catalyst, different olefins (trans-stilbene, cis-cyclooctene, trans-β-methylstyrene and norbornene) were catalyzed using the same experimental procedure.

3. Results and Discussion

3.1. Synthesis of CuO-x NiO/SBA-15 composites.

CuO-x NiO/SBA-15 composites were prepared via ultrasonic post-grafting method. The synthesis SBA-15 was first functionalized with $-CH_3$ and $-NH_2$ on the external and internal surfaces, respectively. The aborption peaks at around 2964 cm^{-1} and 2875 cm^{-1} (Fig. S1) in the FT-IR study indicate the successful grafting of $-CH_3$ and $-NH_2$ on SBA-15 (the content of $-CH_3$ and aminopropyl groups are 8.2 wt% and 6.4 wt%, respectively (Fig. S2)).[31] The modified SBA-15 was then mixed

with the precursor ethanol solution under ultrasonic conditions at room temperature for 4 h. Finally, the products CuO-x NiO/SBA-15 (x = 0, 0.17 and 0.34, x representing the molar ratio of Ni/Cu, according to the ICP analysis) were obtained by calcinations at 550 ℃ for 4 h. The Si-O vibration band in Si-OH around 960 cm^{-1} in Fig. S3 declines and finally disappeares, suggesting CuO loads dispersedly in the channels via bonding with silanols.

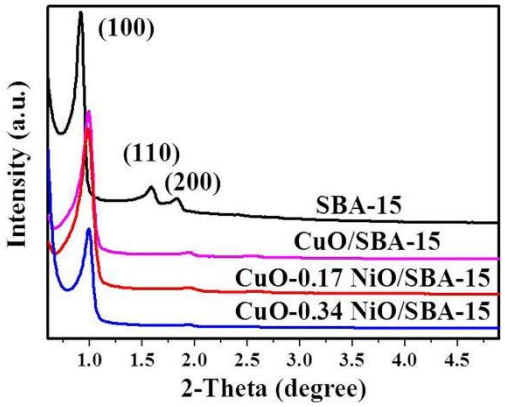

Fig. 1. Small-angle XRD patterns of SBA-15 and CuO-x NiO/SBA-15 (x = 0, 0.17 and 0.34).

Small-angle XRD patterns of SBA-15 and CuO-x NiO/SBA-15 (x = 0, 0.17 and 0.34) are shown in Fig. 1. SBA-15 shows a very sharp d100 diffraction peak (at 2θ = 0.93º) together with two less intense diffraction peaks d110 (at 2θ = 1.60º) and d200 (at 2θ = 1.84º) reflections, indicating the well 2D hexagonal structures of SBA-15.[32] After the metallic oxides were introduced (CuO-x NiO/SBA-15 (x = 0, 0.17 and 0.34)), the intensity of the diffraction peaks becomes weaker and the position changes to lower 2-Theta angle, suggesting the successful introduction of the metal oxides into the mesoporous channels.[33-35]

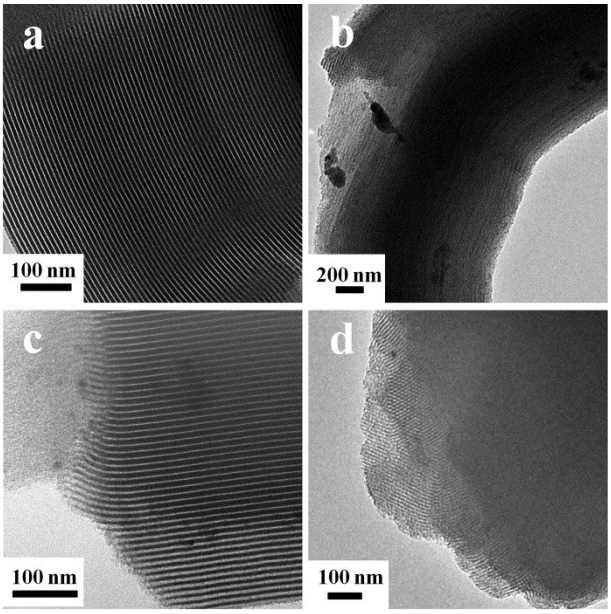

Fig. 2. HRTEM images of (a) pure SBA-15, (b) CuO/SBA-15, (c) CuO-0.17 NiO/SBA-15 and (d) CuO-0.34 NiO/SBA-15.

HRTEM images were determined to study the morphology of SBA-15 and CuO-x NiO/SBA-15 (x = 0, 0.17 and 0.34) (Fig. 2). The pure SBA-15 shows well defined 2D-hexagonal symmetry, and the pore diameter is 6.7 nm (Fig. 2a). After the metallic oxides are loaded, the well-ordered arrays of mesoporous channels of SBA-15 are still preserved (Fig. 2b-d). For CuO/SBA-15, small amounts of large CuO particles are observed on the exterior surface of SBA-15 (Fig. 2b). Compare to the sample prepared using SBA-15 without modification as support shows large amount of CuO particles on the exterior surface of SBA-15 (Fig. S4), the modifications show an active effect for the dispersion of CuO particles in the mesopores. While NiO was added, the large CuO particles disappear gradually and no nucleation of metallic oxide is observed (Fig. 2b-d), this suggests that the addition of small amount of NiO makes CuO disperse uniformly in the mesoporous channels.

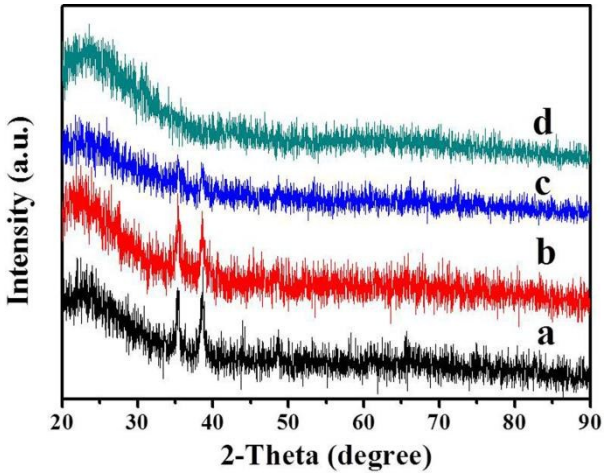

Fig. 3. XRD patterns of (a) CuO/SBA-15, (b) CuO-0.17 NiO/SBA-15, (c) CuO-0.34 NiO/SBA-15 and (d) NiO/SBA-15.

Fig. 3 presents the XRD patterns of CuO-x NiO/SBA-15 (x = 0, 0.17 and 0.34) and NiO/SBA-15. All the samples exhibit a broad band at 23°, which corresponds to the amorphous structure of silica. The CuO peaks for CuO/SBA-15 are found at 35.2 ° and 38.5 °, which correspond to the (002) and (111) of tenorite copper oxide respectively [JCPDS card no. 02-1040]. No obvious peak belonging to NiO is observed in the NiO/SBA-15 (the content of Ni is 5.33 wt%), and the HRTEM image also shows no nucleation of NiO in the channels of SBA-15 (Fig. S5). These results indicate the well dispersion of NiO in the channels.[36] While NiO was introduced into the CuO/SBA-15, CuO-0.17 NiO/SBA-15 exhibits a decrease of characteristic peaks of CuO (the content of Cu is 9.61 wt%), and no characteristic peaks belonging to NiO can be observed. While the content of Ni increases to 0.24 wt% (CuO-0.34 NiO/SBA-15), characteristic peaks of CuO almost disappeared completely, indicating the well dispersal of CuO (the content of Cu is 7.25 wt%). It is suggested that the presence of NiO causes the redistribution of CuO, leading to an enhanced surface content of CuO and the well dispersion of CuO nanoparticles.[35]

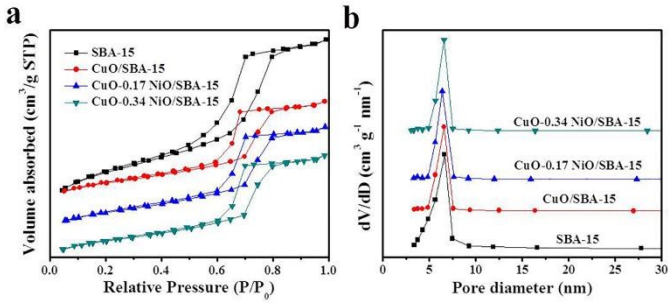

Fig. 4. N_2 adsorption-desorption isotherms (a) and pore sizes distribution (b) of SBA-15 and CuO-x NiO/SBA-15 (x = 0, 0.17 and 0.34).

Table 1. Active phase content and texture properties of SBA-15 and CuO-x NiO/SBA-15 (x = 0, 0.17 and 0.34).

Sample	Cu (wt%)	Ni (wt%)	BET (m^2 g^{-1})	V_p (cm^3 g^{-1})	D_p (nm)
SBA-15	-	-	836.4	0.89	6.63
CuO/SBA-15	10.3	-	444.5	0.57	6.60
CuO-0.17 NiO/SBA-15	9.61	0.16	431.8	0.54	6.39
CuO-0.34 NiO/SBA-15	7.25	0.24	389.0	0.57	6.59

N_2 adsorption-desorption isotherms and the pore sizes distribution of SBA-15 and CuO-x NiO/SBA-15 (x = 0, 0.17 and 0.34) are shown in Fig. 4. All CuO-x NiO-loaded samples exhibit typical type IV for mesoporous structure with H1 hysteresis loops (Fig. 4a), indicating the preservation of ordered mesoporous structure after modifications and incorporating metallic oxide nanoparticles into the channels.[37] The pore sizes distribution calculated by the BJH method of all the samples are showed in Fig. 4b. It can be observed that the desorption pores diameters (Mode) of all composite samples are slightly lower than that of pure SBA-15 (Fig. 4b). The texture properties of the SBA-15 and CuO-x NiO/SBA-15 (x = 0, 0.17 and 0.34) are shown in Table 1. After introducing CuO into the mesopore, the pore size distribution calculated by the BJH method decreases from 6.63 nm for SBA-15 to 6.60 nm for CuO/SBA-15, which is larger than those containing CuO-x NiO in the channels. This suggests that the CuO/SBA-15 with some large CuO particles on the exterior surface of SBA-15 leads to a larger pore size distribution. While the NiO was added, the large CuO particles was dispersed into the channels and caused the decrease of pore size to 6.39 nm for CuO-0.17 NiO/SBA-15. With the increase of the amount of NiO, the dispersion of metallic oxide in the channels leads to the increase of pore size to 6.59 nm for CuO-0.34 NiO/SBA-15. The BET specific surface area decrease from 836.4 m^2 g^{-1} for pure SBA-15 to 444.5 m^2 g^{-1} for CuO/SBA-15, to 431.8 m^2 g^{-1} for CuO-0.17 NiO/SBA-15, and to 389.0 m^2 g^{-1} for CuO-0.34 NiO/SBA-15, respectively. In parallel, the total pore volume decreases from 0.89 cm^3 g^{-1} for SBA-15 to 0.57 cm^3 g^{-1} for CuO/SBA-15, to 0.54 cm^3 g^{-1} for CuO-0.17 NiO/SBA-15, and 0.57 cm^3 g^{-1} for CuO-0.34 NiO/SBA-15, respectively. These may be due to some blocking of the porosity after incorporation of metallic oxides.

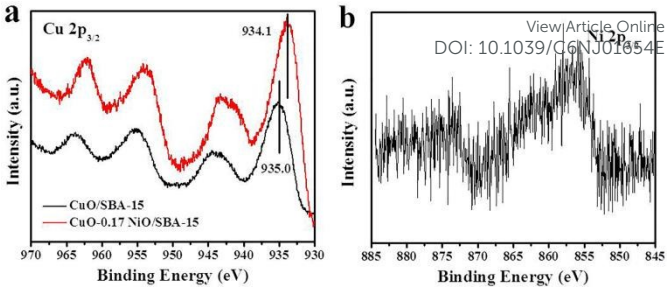

Fig. 5. XPS spectra of (a) Cu 2p3/2 for CuO/SBA-15 and CuO-0.34 NiO/SBA-15, (b) Ni 2p3/2 for CuO-0.34 NiO/SBA-15.

The XPS analysis for a demonstration of the surface chemical states of copper oxide and nickel oxide on CuO/SBA-15 and CuO-0.34 NiO/SBA-15 are shown in Fig. 5. The Cu content of CuO/SBA-15 determined by XPS is 9.8 wt%, which is slightly lower than the ICP result (10.3 wt%), and the Cu and Ni content of CuO-0.34 NiO/SBA-15 are 13.0 wt% and 1.0 wt%, respectively, which are both higher than the analysis by ICP (Cu: 7.25 wt%, Ni: 0.24 wt%). These suggest that the presence of NiO leads to an enhanced surface content of CuO. A feature at 935.0 eV belonging to Cu 2p3/2 appears on CuO/SBA-15, while it shifts to 934.1 eV on CuO-0.34 NiO/SBA-15 (Fig. 5a). Meanwhile, the XPS spectrum of Ni 2p3/2 for CuO-0.34 NiO/SBA-15 at 857.8 eV (Fig. 5b), typical at 852.6 eV for bulk NiO[25], is observed, indicating some interaction between copper and nickel.

3.2. Catalytic properties.

The catalytic activities of CuO-x NiO/SBA-15 (x = 0, 0.17 and 0.34) were evacuated by the epoxidation of styrene at 80 ℃ using TBHP as the oxidant and acetonitrile as the solvent (Table 2). CuO/SBA-15 and NiO/SBA-15 show low activity for this reaction (Table 2, entry 4 and 5), but the introduction of NiO (CuO-0.17 NiO/SBA-15) significantly enhances the conversion of styrene (73.6%) and the selectivity for styrene epoxide (83.2%) (Table 2, entry 6), demonstrating a clear synergistic effect for the NiO-promoted CuO system as compared with the monometallic species. In addition, with the increase of the introduced amount of NiO to 0.34 mol%, the conversion of styrene and selectivity for styrene epoxide increase to 86.2% and 86.3%, respectively, while the physical mixture of NiO/SBA-15 and CuO/SBA-15 shows no obvious enhancement (Table 2, entry 9). Moreover, further increase of the loading amount of NiO does not enhance the conversion of styrene and selectivity for styrene epoxide (Table 2, entry 10).

When small amounts of Na_2CO_3 were introduced, the conversion of styrene reached 100% and the selectivity for styrene epoxide is 92.3% (Table 2, entry 8). By comparison, bare Na_2CO_3 shows a little active for the reaction (Table 2, entry 2). This should be due to the Na_2CO_3 reacting with the radicals on CuO-NiO nanoparticles surface and enhancing the selectivity of styrene epoxide.[38]

View Article Online
DOI: 10.1039/C6NJ01654E

Table 2. Comparison of catalytic activity for the epoxidation of styrene with different as-synthesized catalysts.

Entry	Catalyst	Cu:Ni Molar ratio	Na_2CO_3 (mg)	Conv. (%)	Selec. to epoxide (%)	Yield (%)
1	None	-	-	17.0	74.0	12.6
2	None	-	2.5	43.2	74.8	32.3
3	SBA-15	-	-	21.4	76.1	16.3
4	CuO/SBA-15	1:0	-	66.5	78.8	52.4
5	NiO/SBA-15	0:1	-	26.1	57.8	15.1
6	CuO-0.17 NiO/SBA-15	1:0.17	-	73.6	83.2	61.2
7	CuO-0.34 NiO/SBA-15	1:0.34	-	86.2	86.3	74.4
8	CuO-0.34 NiO/SBA-15	1:0.34	2.5	100	92.3	92.3
9	Mixture of NiO/SBA-15 and CuO/SBA-15	1:0.34	-	64.5	79.1	50.0
10	CuO-NiO/SBA-15	1:1	-	67.4	65.6	44.1

Reaction condition: catalyst containing 0.0129 mmol of CuO, 3 mmol of styrene and 5 mmol of TBHP was stirred in 5 ml of acetonitrile at 80 ℃ for 6h, and nitrobenzene was used as the internal standard.

The stability and cycle performance of the catalyst was investigated. With the CuO-0.34 NiO/SBA-15 catalyst (added Na_2CO_3 into the reaction), the reaction was stopped after 6 h, and the catalyst was collected and reused (Fig. 6a). The recycling results show that the conversion rate maintained at 100% and selectivity of styrene oxide is 86% after cycled 5 times. Furthermore, the catalyst was filtered after 3h reaction, and the liquid phase continued for another 3h, and the conversion shows a slight increase in the absence of catalyst (Fig. 6b). These results show that the catalyst CuO-0.34 NiO/SBA-15 is stable and reusable.

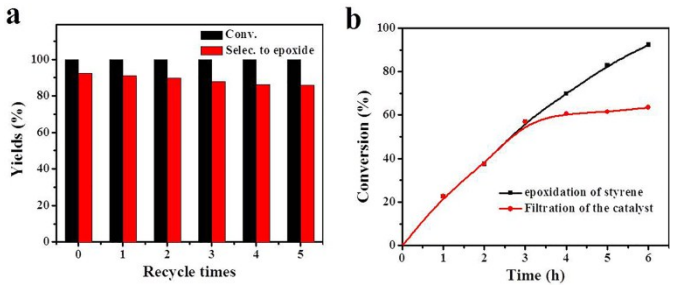

Fig. 6. (a) Recycling results for styrene epoxidation for CuO-0.34 NiO/SBA-15 with Na_2CO_3 added, and (b) leaching experiment.

Table 3. Comparison of the catalytic activity for olefin epoxidation with CuO-0.34 NiO/SBA-15 as catalyst.

Entry	Substrate	Time (h)	Conv. (%)	Selec. to epoxide (%)	Yield
1	cis-cyclooctene	6	84.0	90.3	75.9
2	norbornene	4	81.6	> 99	81.6
3	trans-β-methylstyrene	4	100	> 99	> 99
4	trans-stilbene	3	100	> 99	> 99

In order to investigate the range of adaptability of the CuO-0.34 NiO/SBA-15 catalyst, different olefins including cis-cyclooctene, norbornene, trans-β-methylstyrene and trans-stilbene were selected, and the results are shown in Table 3. After certain times, cis-cyclooctene gives an 84.0% conversion and 90.3% selectivity to epoxycyclooctane, and norbornene shows a desired epoxide in 81.6% yield. Meanwhile, other olefins, such as trans-β-methylstyrene and trans-stilbene have higher epoxide in >99% yield. The reactivity trend (trans-stilbene > trans-β-methylstyrene > norbornene > cis-cyclooctene) indicates the effect of electron-donating groups. It is suggested that substrates with electron-donating are absorbed on the vacant coordination site on the metal oxide surface easily, which makes the double bonds more reactive.[38]

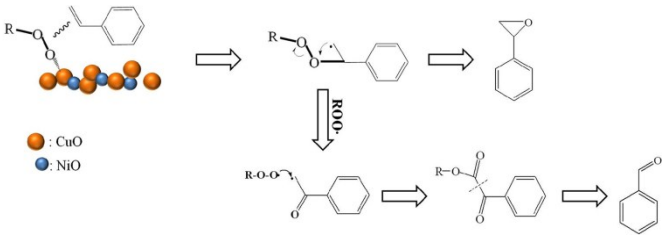

Scheme 1. The possible mechanism of the reaction pathways of styrene.

Based on the above research, the possible mechanism of the reaction pathways of olefins is proposed (Scheme 1). During the catalytic process, the TBHP and substrate are absorbed into the channels, and the adsorbed TBHP is preferentially located on the metal oxide surface, which tends to form peroxidic groups and radicals. The formed peroxidic groups react with the neighboring adsorbed styrene molecules, and insert themselves between the secondary carbons to form the oxametallacycle, and then rearrange to form styrene oxide, while the formed radicals attack the oxametallacycle to get benzaldehyde.[39] The addition of Na_2CO_3, as a hydroxyl radical scavenger, enhances both of the conversion of styrene and selectivity for styrene epoxide. This suggests that the two pathways occur at the same time, and the reaction speed of the epoxidation process is faster.

4. Conclusions

In this paper, NiO promoted CuO-NiO/SBA-15 composites were synthesized using the ultrasonic post-grafting method. With the assistance of $-NH_2$ groups, the precursors were absorbed into the mesoporous channels easily under ultrasonic conditions. The bi-metallic oxides are well-dispersed in very small sizes in the mesoporous channels, and the presence of Ni^{2+} enhances the surface segregation of Cu^{2+}, improving the dispersion of CuO nanoparticles. The electron transfer that occurs between the two metals oxide and good dispersion of active components improve the overall selective epoxidation of olefin with a remarkably high selectivity. In particular, the CuO-0.34 NiO/SBA-15 shows 100% of conversion and 92.3% selectivity for styrene oxide with the addition of Na_2CO_3.

Acknowledgements

We are grateful to the Co-building Special Project of Beijing Municipal Education 111 Project (No. B13004) for financial support of this work.

Notes and references

‡ Electronic Supplementary Information (ESI) available: [FT-IR, TGA and HRTEM of **CuO-x NiO/SBA-15**].

1 J. Hu, *J. Phys. Chem. C*, 2013, **117**, 16005.
2 B. Singh and A. K. Sinha, *J. Mater. Chem. A*, 2014, **2**, 1930.
3 A. Marimuthu, J. W. Zhang and S. Linic, *Science*, 2013, **339**, 1590.
4 R. R. Sever and T. W. Root, *J. Phys. Chem. B*, 2003, **107**, 4090.
5 A. Toshimitsu, H. Abe, C. Hirosawa and S. Tanimoto, *J. Chem. Soc. Chem. Commun.*, 1992, 284.
6 Y. Niibo, T. Nakata, J. Otera and H. Nozaki, *ChemInform*, 1991, **16**, 22.
7 M. Chini, P. Crotti and F. Macchia, *J. Org. Chem.*, 1991, **56**, 5939.
8 Y. Yang, Q. Zhang, T. Shishido and K. Takehira, *J. Catal.*, 2002, **209**, 186.
9 T. J. Terry and P. Stack, *J. Am. Chem. Soc.*, 2008, **130**, 4945.
10 K. Weissermel and H. J. Arpe, *Industrial Organic Chemistry*, 3rd ed.; VCH: Weinheim, Germany, 1997.
11 V. Hulea and E. Dumitriu, *Applied Catalysis A: General*, 2004, **277**, 99.
12 M. Selvaraj, S. W. Song and S. Kawi, *Microporous Mesoporous Mater.*, 2008, **110**, 472.
13 N. Anand, K. H. P. Reddy, V. Swapna, K. S. R. Rao and D. R. Burri, *Microporous Mesoporous Mater.*, 2011, **143**, 132.
14 Y. Luo and J. Lin, *Microporous Mesoporous Mater.*, 2005, **86**, 23.
15 Y. Jin, P. J. Wang, D. H. Yin, J. F. Liu, H. Y. Qiu and N. Y. Yu, *Microporous Mesoporous Mater.*, 2008, **111**, 569.
16 Y. H. Tang, M. Yang, W. J. Dong, L. Tan, X. W. Zhang, P. Zhao, C. H. Peng and G. Wang, *Microporous Mesoporous Mater.*, 2015, **215**, 199.
17 L. P. Xu, S. Sithambaram, Y. S. Zhang, C. H. Chen, L. Jin, R. Joesten and S. L. Suib, *Chem. Mater.*, 2009, **21**, 1253.
18 G. H. Qiu, S. Dharmarathna, Y. S. Zhang, N. Opembe, H. Huang and S. L. Suib, *J. Phys. Chem. C*, 2012, **116**, 468.
19 V. R. Choudhary, R. Jha, N. K. Chaudhari and P. Jana, *Catal. Commun.*, 2007, **8**, 1556.
20 C. Q. Chen, J. Qu, C. Y. Cao, F. Niu and W. G. Song, *J. Mater. Chem.*, 2011, **21**, 5774.
21 A. Miller, B. Zohour, A. Seubsai, D. Noon and S. Senkan, *Ind. Eng. Chem. Res.*, 2013, **52**, 9551.
22 N. Scotti, N. Ravasio, F. Zaccheria, R. Psaro, C. Evangelisti, *Chem. Commun.,* 2013, **49**, 1957.
23 Z. M. Ye, L. Hu, J. Jiang, J. X. Tang, X. Q. Cao and H. W. Gu, *Catal. Sci. Technol.*, 2012, **2**, 1146.
24 X. W. Zhang, G. Wang, M. Yang, Y. Luan, W. J. Dong, R. Dang, H. Y. Gao and J. Yu, *Catal. Sci. Technol.*, 2014, **4**, 3082.
25 A. Ungureanu, B. Dragoi, A. Chirieac, C. Ciotonea, S. Royer, D. Duprez, A. S. Mamede and E. Dumitriu, *ACS Appl. Mater. Interfaces*, 2013, **5**, 3010.
26 C. L. Carnes, J. Stipp and K. J. Klabunde, *Langmuir*, 2002, **18**, 1352.
27 G. Ertl, R. Hierl, H. Knözinger, N. Thiele and H. P. Urbach, *Appl. Surf. Sci.*, 1980, **5**, 49.
28 R. Hierl, H. Knözinger and H. P. Urbach, *J. Catal.*, 1981, **69**, 475.
29 X. B. Huang, M. Yang, G. Wang and X. X. Zhang, *Microporous Mesoporous Mater.*, 2011, **144**, 171.
30 X. W. Zhang, N. Huang, G. Wang, W. J. Dong, M. Yang, Y. Luan and Z. Shi, *Microporous Mesoporous Mater.*, 2013, **177**, 47.
31 X. B. Huang, W. J. Dong, G. Wang, M. Yang, L. Tan, Y. H. Feng and X. X. Zhang, *Journal of Colloid and Interface Science*, 2011, **359**, 40.
32 J. Han, P. Fang, W. J. Jiang, L. Y. Li and R. Guo, *Langmuir*, 2012, **28**, 4768.
33 X. D. Zhang, Z. P. Qu, X. Y. Li, Q. D. Zhao, X. Zhang and X. Quan, *Mater Lett.*, 2011, **65**, 1892.
34 P. V. Adhyapak, P. Karandikar, K. Vijayamohanan, A. A. Athawale and A. J. Chandwadkar. *Mater Lett.*, 2004, **58**, 1168.
35 J. Blanco, P. Avila, S. Suárez, M. Yates, J. A. Martin, L. Marzo and C. Knapp, *Chemical Engineering Journal*, 2004, **97**, 1.
36 C. Huang, Y. C. Chung and M. R. Liou, *Journal of Hazardous Materials*, 1996, **45**, 265.
37 M. Kruk and M. Jaroniec, *Chem. Mater.*, 2001, **13**, 3169.
38 Y. Yang, J. Ma, Q. Qin and X. J. Zhai, *J. Mol. Catal. A: Chem.*, 2007, **276**, 41.
39 R. A. Sheldon, *Rec. Trav. Chim. Pays-Ba*, 1973, **92**, 253.
40 L. Zhou and R. J. Madix, *J. Phys. Chem. C*, 2008, **112**, 4725.

View Article Online
DOI: 10.1039/C6NJ01654E

View Article Online
DOI: 10.1039/C6NJ01654E

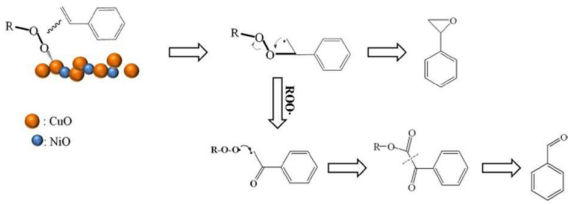

NiO promoted the well dispersion of CuO in the CuO-NiO/SBA-15 composites, which showed high activity for the epoxidation of olefins.